Nuclear Medicine and Molecular Imaging (2019) 53:414–422
https://doi.org/10.1007/s13139-019-00619-5

ORIGINAL ARTICLE

ISSN (print) 1869-3482
ISSN (online) 1869-3474

Effect of ME Collimator Characteristic, Energy Window Width, and Reconstruction Algorithm Selection on Imaging Performance of Yttrium-90: Simulation Study

Payvand Taherparvar[1] · Nazila Shahmari[1]

Received: 8 June 2019 / Revised: 24 September 2019 / Accepted: 17 October 2019 / Published online: 13 November 2019

Abstract

Purpose The treatment efficiency of ^{90}Y and providing reliable estimates of activity are evaluated by SPECT imaging of bremsstrahlung radiation released during beta therapy. In this technique, the resulting spectrum from ^{90}Y is very complex and continuous, which creates difficulties on the imaging protocol. Moreover, collimator geometry has an impressive effect on the spatial resolution, system sensitivity, image contrast, and the signal-to-noise ratio (SNR), which should be optimized.

Methods We evaluated the effect of energy window width, reconstruction algorithms, and different geometries of a medium-energy (ME) parallel-hole collimator on the image contrast and SNR of ^{90}Y SPECT images. The Siemens E.Cam gamma camera equipped with a ME collimator and a digital Jaszczak phantom were simulated by SIMIND Monte Carlo program to generate the ^{90}Y bremsstrahlung SPECT images.

Results Our results showed that optimal image quality can be acquired by the reconstruction algorithm of OS-EM in the energy window width of 60 to 400 keV for ^{90}Y bremsstrahlung SPECT imaging. Furthermore, the optimal values of the hole diameter and hole length of a ME collimator were obtained 0.235 and 4.4 cm, respectively.

Conclusions The acquired optimal ME collimator and energy window along with using a suitable reconstruction algorithm lead to improved contrast and SNR of ^{90}Y bremsstrahlung images of hot spheres of the digital Jaszczak phantom. This can improve the accuracy and precision of the ^{90}Y activity distribution estimation after radioembolization in targeted radionuclide therapy.

Keywords Yttrium-90 · SPECT · Energy window · Collimator · Contrast · SNR · SIMIND

Introduction

Because of its chemistry, the energy of β-particle emitted during radioactive decay, and a proper half-life (64.1 h) of yttrium-90 (^{90}Y), it is used clinically in targeted radionuclide therapy (TRT) for therapeutic treatments of malignant diseases such as non-Hodgkins lymphoma and metastatic liver tumors (via microsphere radioembolization) [1, 2]. Recently, radiation therapy treatment efficiency based on the ^{90}Y bremsstrahlung single photon emission computed tomography (SPECT) imaging has been considered to provide reliable estimates of the activity distribution and subjective improvement in diagnostic accuracy and image quality [1, 3]. In the ^{90}Y SPECT imaging, as a result of the interaction of β-particles with the patient's tissues, the bremsstrahlung photons are created. Unlike conventional radioisotopes used for diagnostic imaging, energy distribution of the ^{90}Y bremsstrahlung photons is very complex and extended up to energies around 2.3 MeV, which increases the demands on the SPECT protocol such as energy window width, collimator selection, and image reconstruction [4–6]. The collimator is one of the critical components in SPECT imaging and in the performance of a scintillation camera. To obtain an image with a scintillation gamma camera, it is necessary to project gamma rays from the patient tissue to the camera detector. The walls between the collimator holes and septa absorb most photons that are scattered by an object and do not emanate from the direction of interest. This is one of the important reasons for the relatively poor image quality of radionuclide imaging, which can affect the system sensitivity and so the

✉ Payvand Taherparvar
p.taherparvar@guilan.ac.ir; p.taherparvar@gmail.com

[1] Faculty of Science-Physics Department, University of Guilan, Namjoo Avenue, Rasht, Guilan 4193833697, Iran

reliability of activity estimation [2, 5, 7]. Therefore, the choice of a collimator with appropriate geometric structure is one of the most important factors to optimize the image quality. Clinically, high-energy (HE) or medium-energy (ME) parallel-hole collimators are currently used for ^{90}Y bremsstrahlung SPECT imaging. Noting that these collimators are specially designed for high-energy isotopes with complex energy distribution, such as multiple energy peaks, e.g., gallium-67 or iodine-131 [2, 8]. In ^{90}Y imaging, penetration and scattering of the bremsstrahlung photons through the septa are other reasons for the poor image quality. Thus, collimators with a small level of scattered radiation and photons penetration through their septa are preferable for bremsstrahlung SPECT imaging [2]. Generally, the performance of parallel-hole collimators is influenced by their geometry such as collimator thickness, hole diameter, and septa thickness [9], which affects the image quality, system sensitivity, and activity distribution evaluation in the ^{90}Y bremsstrahlung SPECT imaging [5].

On the other hand, the reconstruction algorithm is the other important factor in the computed tomography imaging [6]. 3-D image of the activity distribution can be achieved noninvasively using tomographic acquisition and the image reconstruction techniques [10]. The reconstruction methods are generally divided into analytic methods such as the filter back projection (FBP) and iterative methods such as maximum likelihood expectation maximization (ML-EM), and ordered subsets expectation maximization (OS-EM) algorithms. Although the FBP algorithm is faster compared with iterative algorithms, iterative methods demonstrate the better image quality and accurate modeling of the emission than the FBP method. As compared with the ML-EM, OS-EM algorithm needs less computation time, which with having the current computational power of modern computers will be feasible for routine clinical use [11]. In SPECT imaging, it has been demonstrated that OS-EM method gives fewer artifacts in reconstructed images than FBP algorithm [12, 13]. In addition, the OS-EM iterative reconstruction algorithm improves the quantitative accuracy of ^{90}Y SPECT and eliminates streak artifact compared with FBP reconstruction algorithm [14].

Numbers of studies have been done to optimize the reconstruction parameters, energy window width, and geometry of collimator for ^{90}Y bremsstrahlung SPECT imaging. The effect of the variation of the hole diameter of a ME collimator (for given septa and collimator thickness) in three energy window width was investigated by Roshan et al. on the contrast of ^{90}Y SPECT images to achieve a better image quality [9]. Rong et al. have developed a method for energy window optimization in quantitative imaging of ^{90}Y SPECT when bias is a vital element limiting reliability [15]. Roshan et al. also provided a review of the optimization methods of factors such as the energy window, collimator, and reconstruction algorithm for ^{90}Y bremsstrahlung SPECT imaging to optimize the treatment efficacy of liver tumor radioembolization using ^{90}Y microspheres [16]. Kim et al. presented a universal condition for the selection of the energy window width and collimator type by investigation of Monte Carlo (MC) simulation of bremsstrahlung images for the better acquisition of ^{90}Y imaging [17]. Walrand et al. optimized an Anger camera–collimator system for ^{90}Y bremsstrahlung SPECT imaging by use of Monte Carlo simulations [5]. McQuaid et al. improved the collimator and reconstruction parameters in SPECT imaging for lesion quantification [6]. Leong et al. evaluated the uniformity requirements for image reconstruction in SPECT imaging using FBP and OS-EM reconstruction techniques [13]. Furthermore, the other studies have been done to improve the collimator and reconstruction algorithms for evaluation of the quantitative accuracy in the ^{90}Y bremsstrahlung SPECT imaging [1, 2, 14]. But until now, optimization of the thickness and hole diameter of a parallel-hole collimator have never been assessed simultaneously, for ^{90}Y bremsstrahlung SPECT imaging. In this paper, we used SIMIND Monte Carlo simulation program to investigate the influences of hole diameter and thickness of a ME collimator currently used for clinical ^{90}Y imaging. Moreover, we studied the effects of energy window width and image reconstruction methods on the image quality of bremsstrahlung imaging by some criteria such as image contrast and SNR.

Material and Methods

Monte Carlo Simulation and Image Generation

We used the simulated Siemens E.CAM SPECT imaging system by the Monte Carlo simulation code, SIMIND version 6.1.1, which has been developed by Michael Ljungberg [18, 19], to generate the ^{90}Y bremsstrahlung images. Monte Carlo simulation provides a powerful means for validation and optimization of medical imaging systems [20] and radiation therapy (radiotherapy) techniques [21, 22]. Many dedicated Monte Carlo codes, such as GATE [22], SimSET [23], and SIMIND [18], have been developed and applied for nuclear medicine imaging research. The SIMIND Monte Carlo code defines a clinical SPECT camera and can be modified for different type of calculation in the SPECT systems [18]. We validated the SIMIND code for ^{90}Y SPECT imaging according to the earlier surveys [4, 9].

In order to evaluate the contrast and SNR, we used a Jaszczak cylindrical uniform source phantom established by Islamian et al. [24]. The phantom consist of six hot spheres in different diameters: 9.5, 12.7, 15.9, 19.1, 25.4, and 31.8 mm. The phantom was located in the center of the field of view at a distance of 15 cm from the collimator lower surface of the simulated gamma camera. Total activity of 1.5 GBq ^{90}Y was considered for the hot spheres of Jaszczak phantom without background activity. One hundred twenty-eight projections

were acquired in 128 × 128 matrix with a pixel size of 0.4 cm over 360° counter-clockwise rotations. Acquisition time was about 25 s per projection with 1.5 million counts per projection. Because of the energy range effect of bremsstrahlung photons on their attenuation in the body's tissues and their generation from the collimator septa penetration and scattering, we chose two energy windows including energy windows ranging from 60 to 160 keV (a narrow energy window) and 60 to 400 keV (the extended energy window).

We used the ME collimator of the Siemens E.Cam gamma-camera. In SPECT imaging, spatial resolution is limited via the collimator resolution [25]. The geometric resolution of the parallel-hole collimators with hexagonal holes (R_{coll}) can be expressed as:

$$R = \sqrt{2\ln 2}\ \frac{D}{T}(F + T) \quad (1)$$

where T, D, and F indicate the hole length, hole diameter (flat-to-flat distance for hexagonal holes), and the distance from the imaged object to the detector surface, respectively [2]. In order to optimize the ME collimator for ^{90}Y bremsstrahlung SPECT imaging, the values of R_{coll} were considered between 1 and 1.8 cm as recommended by Rong et al. [2] for a distance of 15 cm between the source and the collimator surface. To achieve the values of R_{coll} between 1 and 1.8 cm, we chose the hole diameter (D) values of 2.35, 2.59, 2.82, 2.94, 3.06, and 3.3 mm, and also the hole length (T) values of 3, 3.2, 3.4, 3.6, 3.8, 4, 4.2, and 4.4 cm for a ME collimator without changing septa thicknesses (1.14 mm).

Since in the case of bremsstrahlung imaging, the iterative methods are widely utilized for image reconstruction [4], images were reconstructed by OS-EM algorithm with 200 iterations and 16 subsets. The projections were also reconstructed by FBP method using Shepp-Logan filter with a cut-off frequency of 0.5 cycles per pixel, which was chosen according to Roshan et al. [9] study, using MATLAB program. In both reconstruction method, acquired phantom images were set to a voxel size of 4 × 4 × 4 mm^3.

To evaluate the quality of the reconstructed ^{90}Y SPECT images, the image contrast and SNR of hot spheres were studied. Image contrast was calculated for the six hot spheres of the Jaszczak phantom by using following equation:

$$C_l = \frac{R_l - R_0}{R_0} \quad (2)$$

where R_l is the mean pixel values for activity inside hot spheres and R_0 is the mean pixel values for activity of background. To measure R_l, a circular region of interest (ROI) was defined around the center of multiple spheres of various sizes on the reconstructed images. The ROI sizes were set according to the sizes of simulated multiple spheres. Moreover, to measure R_o, an arbitrary ROI excluding the ROIs belonging to the hot spheres was defined in the background on the reconstructed image, as shown in Fig. 1. In this way, the number of the voxels included in the ROIs was about 130, 78, 54, 40, 26, and 14 for the largest to the smallest spheres, respectively. Moreover, the number of the voxels included in the background ROI was about 130.

The SNR values in the reconstructed images were calculated by following formula:

$$SNR = \frac{N_S - N_{BG}}{\sigma_{BG}} \quad (3)$$

where N_S and N_{BG} are the count density in the ROI in the central region of multiple spheres and background, respectively, and σ_{BG} is the standard deviation of the values for the background activity.

Results

In this paper, the effect of the geometric structure of a ME parallel-hole collimator (i.e., hole length and hole diameter, without changing the septa thicknesses) and energy window width (60 to 160 keV as a narrow energy window and 60 to 400 keV as an extended energy window) were evaluated on the image contrast and SNR of bremsstrahlung images of hot spheres of Jaszczak phantom using the SIMIND Monte Carlo program.

Image reconstruction has significant impacts on the image quality in the ^{90}Y bremsstrahlung SPECT imaging due to the broad energy spectrum of the related bremsstrahlung photons. Hence, in this paper, by use of the image contrast and SNR criteria, we compared the image quality of reconstructed spheres images of the simulated Jaszczak phantom, which

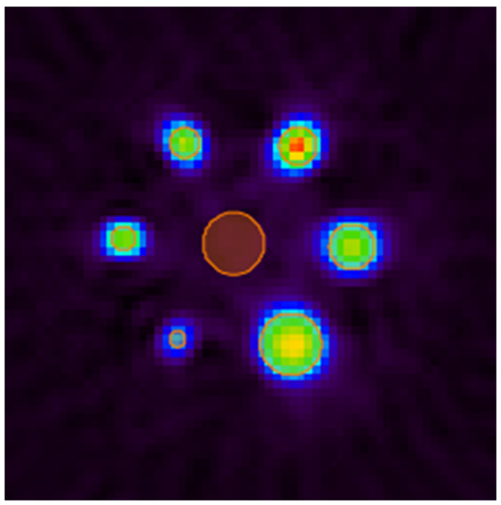

Fig. 1 Reconstructed image of hot spheres of a Jaszczak phantom, along with 7 ROIs: six ROIs for hot spheres of Jaszczak phantom along with background ROI

were acquired with two reconstruction algorithms including FBP (with a Shepp-Logan filter) and OS-EM.

Figures 2 and 3 show the effects of the energy window width and geometric structure of the parallel-hole collimator including the hole length and hole diameter on the image contrast of six hot spheres with different diameters for ^{90}Y bremsstrahlung SPECT imaging. These images were reconstructed using the FBP algorithm with the Shepp-Logan filter. As can be seen in these figures, in comparison with the narrow energy window (60–160 keV) (Fig 3), the image contrast for all spheres was improved by using the extended energy window (60–400 keV) (Fig 2). Results were same for all spheres of the Jaszczak phantom. On the other hand, the contrast of spheres images was also increased with increasing the hole length for a specific hole diameter. Furthermore, for a specific hole length, with increasing the hole diameter, the contrast of images was decreased.

Figure 4 shows the results of the image contrast of the spheres images, which were reconstructed with the OS-EM algorithm. Comparison of the contrast diagrams for six hot spheres with different diameters in Figs. 2 and 4 indicates that the reconstructed images by OS-EM algorithm appear to have higher contrast than the reconstructed spheres images by FBP. The variation of the contrast values of hot spheres images versus the hole diameter and hole length of the parallel-hole collimator follows the same curves for reconstructed images by two algorithm methods. Results indicate that the best contrast was obtained by using the hole diameter of 0.235 cm and hole length of 4.4 cm. Further, a better and more accurate measure was achieved for the sphere with larger diameter.

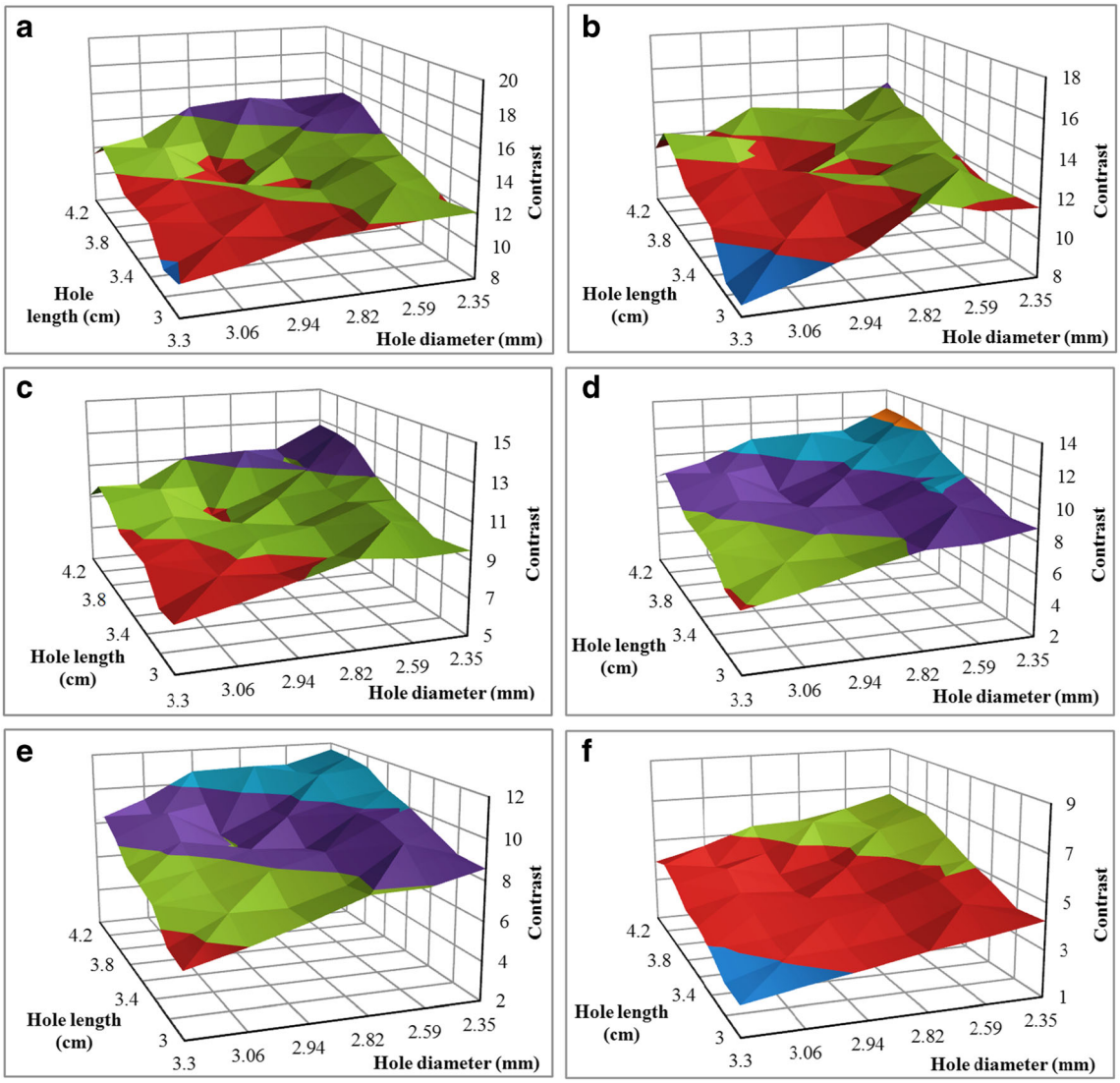

Fig. 2 The image contrast of hot spheres of a Jaszczak phantom (with different diameters of 31.8 (**a**), 25.4 (**b**), 19.1 (**c**), 15.9 (**d**), 12.7 (**e**), and 9.5 (**f**) mm) from the ^{90}Y bremsstrahlung SPECT imaging as a function of hole diameter and hole length of a parallel-hole collimator in the energy window width of 60–400 keV. The images were reconstructed using the FBP algorithm with a Shepp-Logan filter

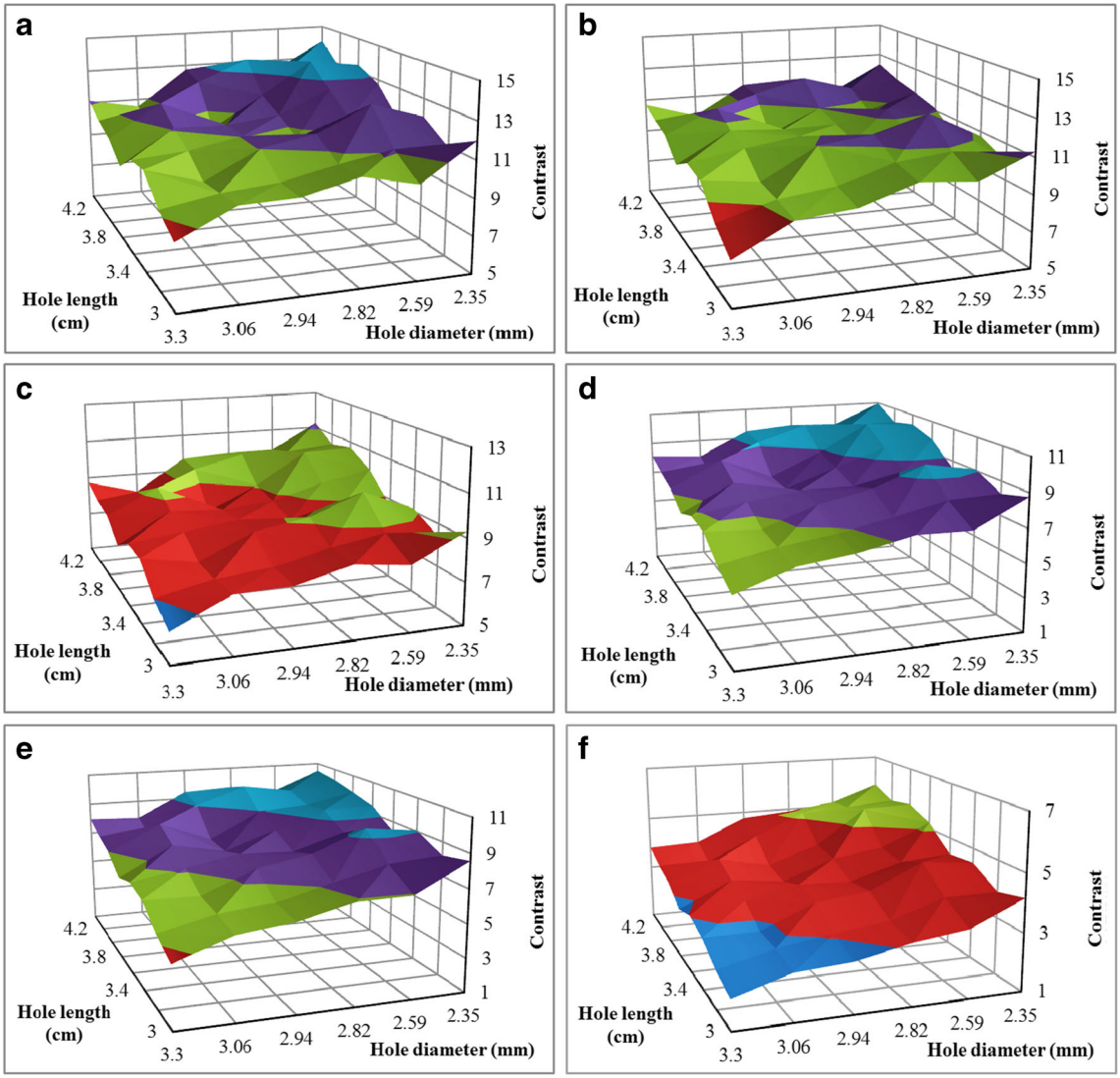

Fig. 3 The image contrast of hot spheres of a Jaszczak phantom (with different diameters of 31.8 (**a**), 25.4 (**b**), 19.1 (**c**), 15.9 (**d**), 12.7 (**e**), and 9.5 (**f**) mm) from the ^{90}Y bremsstrahlung SPECT imaging as a function of hole diameter and hole length of a parallel-hole collimator in the energy window width of 60–160 keV. The images were reconstructed using the FBP algorithm with a Shepp-Logan filter

For further analysis, we evaluated the bremsstrahlung photons penetration and scattering in the collimator septa in the best energy window width (60–400 keV). The results were listed in Table 1. As can be seen in Table 1, with increasing the hole length and decreasing the hole diameter, penetration and scattering of ^{90}Y bremsstrahlung photons through the collimator septa were decreased. The collimator with the hole diameter of 0.235 cm and hole length of 4.4 cm has small level of penetration and scattering through the septa in energy window of 60–400 keV (Table 1). For visual comparison, the spheres images of the simulated Jaszczak phantom in energy window width of 60–160 keV and 60–400 keV, which were reconstructed with the FBP algorithm, are shown in Fig. 5 a and b, respectively. Furthermore, Fig. 5c shows the reconstructed images of spheres by OS-EM algorithm in the optimal energy window width (60–400 keV). In comparison with the reconstructed images by FBP, efficient noise reduction and achieving a suitable image quality are seen in the reconstructed images by OS-EM algorithm.

We calculated SNR values of six hot spheres images of the Jaszczak phantom as a function of hole diameter and hole length of a parallel-hole collimator in the two energy windows. The results of our study show that the SNR values were increased with increasing the hole length and decreasing the hole diameter, which are similar to the results of contrast analysis. The results demonstrate that the best SNR was obtained by using the wide energy window of 60 to 400 keV. Table 2 shows the SNR values of reconstructed images by two reconstruction algorithms (FBP and OS-EM) for the selected optimal parallel-hole collimator (hole diameter of 0.235 and hole length of 4.4 cm), in the best energy window width. The results show the superiority of OS-EM with respect to FBP

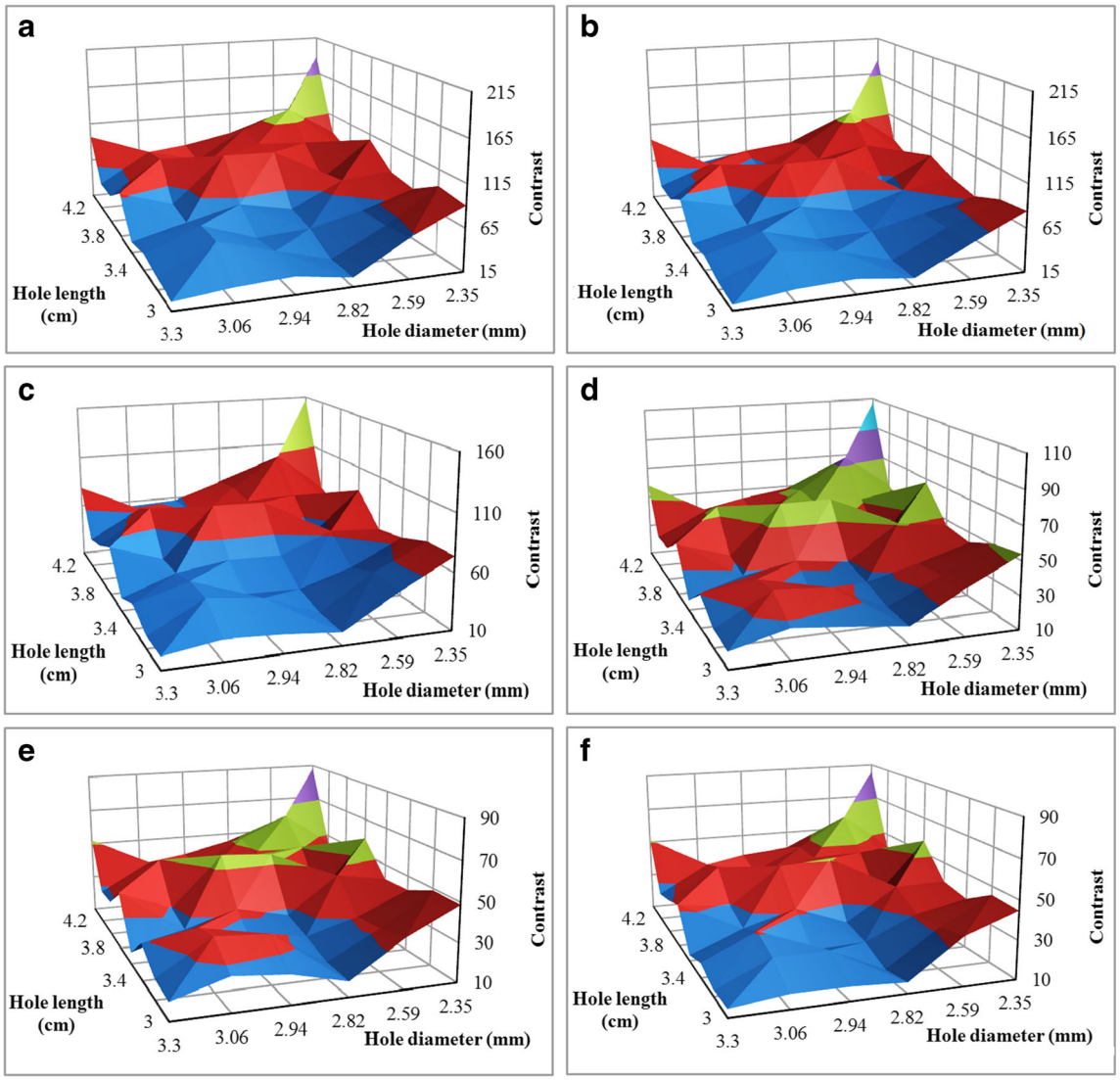

Fig. 4 The image contrast of hot spheres of a Jaszczak phantom (with different diameters of 31.8 (**a**), 25.4 (**b**), 19.1 (**c**), 15.9 (**d**), 12.7 (**e**), and 9.5 (**f**) mm) from the ^{90}Y bremsstrahlung SPECT imaging as a function of hole diameter and hole length of a parallel-hole collimator in the energy window width of 60–400 keV. The images were reconstructed using the OS-EM algorithm

in terms of SNR calculation. Moreover, the hot sphere with a larger diameter has a higher SNR value than others.

Discussion

Because of the absence of a pronounced photopeak energy of bremsstrahlung photons, the quality of ^{90}Y bremsstrahlung SPECT images of patients treated with ^{90}Y is poor [16]. In the energy spectrum of the ^{90}Y bremsstrahlung photons, since the most photons with energies lower than 60 keV are attenuated in the patient's tissue and higher than 500 keV are penetrated in the collimator septa, the optimum energy window should be set inside this limit, which affects the system sensitivity subsequently [3, 15]. Since the image contrast in the nuclear medicine imaging is difference in intensity between regions of the imaged object containing different concentrations of activity [7], measurement of image contrast is a good criterion for accurate activity concentration. Furthermore, the SNR also is a frequently used metric of image evaluation, measurement of contrast enhancement, and quality assurance [26].

In this study, we studied the effect of different parameters such as the energy window width, collimator characteristic (i.e. hole diameter, hole length, and septa thickness), and different reconstruction methods on the image contrast and SNR of bremsstrahlung SPECT images of six hot spheres of Jaszczak phantom. According to the obtained results, the image contrast and SNR have been increased by use of the wide energy window ranging from 60 to 400 keV, which is applicable for clinical scanning. Further, a wide energy window causes to increasing the system sensitivity and decreasing

Table 1 Fraction of photon penetration and scattering in the collimator septa in the best energy window width (60–400 keV) and septa thicknesses of 0.114 cm for different values of hole length and fixed hole diameter of 0.235 cm (left) and different values of hole diameter and fixed hole length of 4.4 cm (right)

Hole diameter = 0.235 cm			Hole length = 4.4 cm		
Hole length (cm)	Penetration	Scatter	Hole diameter (cm)	Penetration	Scatter
3	5.99%	3.27%	0.235	4.05%	2.78%
3.2	5.58%	3.19%	0.259	4.06%	2.82%
3.4	5.29%	3.11%	0.282	4.06%	2.82%
3.6	4.99%	3.02%	0.294	4.07%	2.83%
3.8	4.70%	2.96%	0.306	4.07%	2.84%
4	4.46%	2.91%	0.33	4.08%	2.85%
4.2	4.24%	2.84%	-----	-----	-----
4.4	4.05%	2.78%	-----	-----	-----

the bias and also variance of the activity estimation in the ^{90}Y bremsstrahlung SPECT imaging [15]. In the ^{90}Y SPECT imaging, penetration and scattering of the bremsstrahlung photons through the collimator septa are the image-degrading effects [2]. Therefore, the choice of a collimator with the suitable geometry along with the minimal scattered radiation and photons penetration through the septa leads to correct estimation of activity during radiation therapy and by that can be achieved a better image quality of ^{90}Y bremsstrahlung SPECT images. For this purpose, the applied studies for the collimator with different hole diameters and lengths, which their resolutions were detected between 1 and 1.8 cm, indicated that the better results for the image contrast and SNR can be obtained by using the collimators with larger hole length and smaller hole diameter, which generate the least penetration and scattering. Although Roshan et al. [9] mentioned that the contrast of reconstructed images by FBP algorithm can be increased by increasing the hole diameter and energy window width for fixed collimator and septa thickness values, our results for different values of hole length and hole diameter indicated that image quality can be also increased by decreasing the hole diameter, while R_{coll} was considered between 1 and 1.8 cm. The reconstruction algorithm is another factor with a significant effect on the image quality in the ^{90}Y bremsstrahlung SPECT imaging. For this purpose, the image quality of the simulated images, which were reconstructed by two reconstruction algorithms including the FBP and OS-EM, was evaluated by using the contrast and SNR as quality metrics. The results showed that the OS-EM reconstruction method yields higher contrast and SNR and better image quality than FBP in all cases, although the OS-EM reconstruction process significantly increases the image reconstruction time. Achieving the images with high contrast and SNR and also the smallest level of scattered radiation and penetration of bremsstrahlung photons through the collimator septa can improve the estimation of ^{90}Y microsphere activity distribution in bremsstrahlung SPECT imaging after radiation therapy and treatment efficacy.

Conclusion

We investigated the effects of the energy window width, the geometric structure of a ME parallel-hole collimator and the reconstruction algorithm on the images contrast and SNR of ^{90}Y bremsstrahlung SPECT by SIMIND Monte Carlo simulation program. The results showed that the best contrast and SNR are obtained by use of an wide energy window ranging from 60 to 400 keV as the optimal energy window and a ME collimator with a hole diameter of 0.235 cm, a hole length of 4.4 cm, and a septa thicknesses of 0.114 cm as the optimal geometric structure of collimator, which leads to the minimum

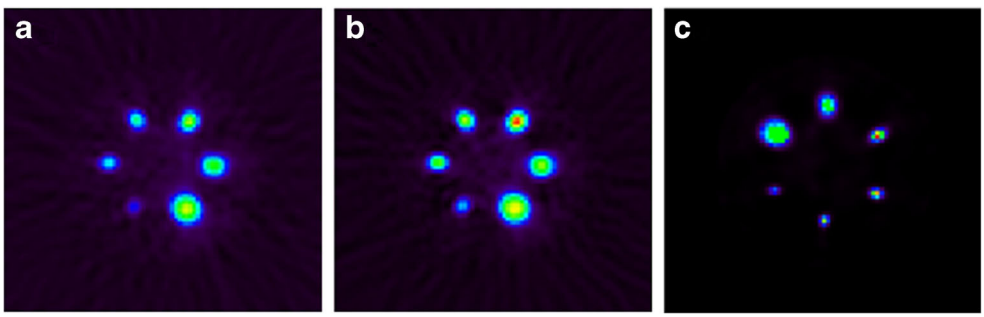

Fig. 5 The reconstructed images of six hot spheres of Jaszczak phantom by use of the FBP algorithm in energy window widths of 60–160 keV (**a**) and 60–400 keV (**b**) and use of the OS-EM algorithm in energy window width of 60–400 keV (**c**)

Table 2 The SNR values of hot spheres images reconstructed by two reconstruction algorithms of FBP and OS-EM, which were obtained for an optimal parallel-hole collimator with a hole diameter and hole length of 0.235 and 4.4 cm, respectively, in the energy window width of 60–400 keV

Sphere diameter (mm)	SNR	
	FBP	OS-EM
31.8	102.4867	342.2905
25.4	86.18134	336.5994
19.1	83.7091	285.6996
15.9	83.13094	195.5808
12.7	74.66184	160.6191
9.5	43.63119	155.9509

scattering and photons penetration through the septa, along with the reconstruction algorithm of OS-EM, which can improve the reconstructed images quality and present the better activity estimation in the SPECT images of ^{90}Y.

Acknowledgments The authors would like to thank Professor Michael Ljungberg for providing the valuable advices.

Compliance with Ethical Standards

Conflict of Interest Payvand Taherparvar declares that he has no conflict of interest. Nazila Shahmari declares that she has no conflict of interest.

Ethical Approval This article does not contain any studies with human participants or animals performed by any of the authors.

Informed Consent The institutional review board of our institute approved this retrospective study, and the requirement to obtain informed consent was waived.

References

1. Minarik D, Gleisner KS, Ljungberg M. Evaluation of quantitative 90-Y SPECT based on experimental phantom studies. Phys Med Biol. 2008;53:5689–703.
2. Rong X, Frey EC. A collimator optimization method for quantitative imaging: application to Y-90 bremsstrahlung SPECT. Med Phys. 2013;40:1–9.
3. Rong X, Ghaly M, Frey EC. Optimization of energy window for ^{90}Y bremsstrahlung SPECT imaging for detection tasks using the ideal observer with model-mismatch. Med Phys. 2013;40:062502.
4. Rong X, Du Y, Ljungberg M, Rault E, Vandenberghe S, Frey EC. Development and evaluation of an improved quantitative 90-Y bremsstrahlung SPECT method. Med Phys. 2012;39:2346–58.
5. Walrand S, Hesse M, Wojcik R, Lhommel R, Jamar F. Optimal design of Anger camera for bremsstrahlung imaging: Monte Carlo evaluation. Front Oncol. 2014;4:1–7.
6. McQuaid SJ, Southekal S, Kijewski MF, Moore SC. Joint optimization of collimator and reconstruction parameters in SPECT imaging for lesion quantification. Phys Med Biol. 2011;56:6983–7000.
7. Chery SR, Sorenson JA, Phelps ME. Physics in Nuclear Medicine. Elsevier/Saunders. Philadelphia; 2012.
8. Bonutti F, Avolio M, Magro G, Cecotti A, Della Schiava E, Del Dò E, et al. Optimization of the image contrast in SPECT-CT bremsstrahlung imaging for selective internal radiation therapy of liver malignancies with Y-90 microspheres. arXiv preprint arXiv: 1509.08857. 2015;1-13.
9. Rezaei Roshan H, Azarm AR, Mahmoudian B, Gharepapagh E, Islamian J. Collimator and energy window optimization for Y-90 bremsstrahlung SPECT imaging: a SIMIND Monte Carlo study. Appl Radiat Isot. 2016;108:124–8.
10. Sadremomtaz A, Taherparvar P. The influence of filters on the SPECT image of Carlson phantom. J Biomed Sci Eng. 2013;6: 291–7.
11. Bruyant PP. Analytic and iterative reconstruction algorithms in SPECT. J Nucl Med. 2002;43:1343–58.
12. Hatton RL, Hutton BF, Angelides S, Choong KK, Larcos G. Improved tolerance to missing data in myocardial perfusion SPET using OS-EM reconstruction. Eur J Nucl Med Mol Imaging. 2004;31:857–61.
13. Leong LK, Kruger RL, O'Connor MK. A comparison of the uniformity requirements for SPECT image reconstruction using FBP and OS-EM techniques. J Nucl Med Technol. 2001;29:79–83.
14. Ahmadzadehfar H, Muckle M, Sabet A, Wilhelm K, Kuhl C, Biermann K, et al. The significance of bremsstrahlung SPECT/CT after yttrium-90 radioembolization treatment in the prediction of extrahepatic side effects. Eur J Nucl Med Mol Imaging. 2012;39: 309–15.
15. Rong X, Du Y, Frey EC. A method for energy window optimization for quantitative tasks that includes the effects of model-mismatch on bias: application to Y-90 bremsstrahlung SPECT imaging. Phys Med Biol. 2012;57:3711–25.
16. Rezaei Roshan H, Azarm AR, Mahmoudian B, Islamian J. Advances in SPECT for optimizing the liver tumors radioembolization using yttrium-90 microspheres. World J Nucl Med. 2015;14:75–80.
17. Kim M, Bae JK, Hong BH, Kim KM, Lee W. Effects of collimator on imaging performance of yttrium-90 bremsstrahlung photons: Monte Carlo simulation. Nucl Eng Technol. 2019;51:539–45.
18. Ljungberg M. The SIMIND Monte Carlo program. Monte Carlo Calculations in Nuclear Medicine: Applications in Diagnostic Imaging. 2012. pp. 111-28.
19. Toossi MB, Islamian JP, Momennezhad M, Ljungberg M, Naseri S. SIMIND Monte Carlo simulation of a single photon emission CT. J Med Phys/Assoc Med Phys India. 2010;35:42.
20. Taherparvar P, Sadremomtaz A. Development of GATE Monte Carlo simulation for a CsI pixelated gamma camera dedicated to high resolution animal SPECT. Australas Phys Eng Sci Med. 2018;41:31–9.
21. Rajabi R, Taherparvar P. Monte Carlo dosimetry for a new 32P brachytherapy source using FLUKA code. J Contemp Brachyther. 2019;11:76–90.
22. Fardi Z, Taherparvar P. A Monte Carlo investigation of the dose distribution for new I-125 low dose rate brachytherapy source in water and in different media. Polish J Med Phys Eng. 2019;25:15–22.
23. http://depts.washington.edu/simset/html/simset_main.html. Accessed 18 May 2019.

24. Islamian JP, Bahreyni Toossi MT, Momennezhad M, Naseri S, Ljungberg M. Simulation of a quality control Jaszczak Phantom with SIMIND monte carlo and adding the phantom as an accessory to the program. Iran J Med Phys. 2012;9:135–40.
25. Smith MF, Majewski S, Weisenberger AG. Optimizing pinhole and parallel hole collimation for scintimammography with compact pixellated detectors. Nucl Sci IEEE Trans. 2003;50:321–6.
26. Dietrich O, Raya JG, Reeder SB, Reiser MF, Schoenberg SO. Measurement of signal-to-noise ratios in MR images: influence of multichannel coils, parallel imaging, and reconstruction filters. J Magn Reson Imaging. 2007;26:375–85.